PERGAMON

Chemical Engineering Science 58 (2003) 1831–1837

Chemical Engineering Science

www.elsevier.com/locate/ces

A torque-based analysis of the reverse roll coating process

S. Alonso[1], F. Bertrand, P. A. Tanguy*

NSERC-Paprican Chair/URPEI, Department of Chemical Engineering, École Polytechnique, P.O. Box 6079, Station Centre-Ville, Montreal, Canada H3C 3A7

Received 11 October 2001; received in revised form 5 September 2002; accepted 1 October 2002

Abstract

In a laboratory film coater operated at industrial speed, the torque exerted by the metering rod was used to investigate the hydrodynamics in the metering nip flow. CFD simulations were also performed taking into account the deformation of the roll cover to depict the elastohydrodynamics of the metering nip flow. From the experiments, it was found that the torque increases with transfer speed, load and viscosity. When runnability problems such as spitting were observed, the torque signal decreased. Torque measurements could also predict excessive friction between rod and roll, which may damage the elastic cover. The numerical simulations showed trends similar to the experiments. Regions of positive and negative torque values demonstrated how the fluid interacts with the rod, a phenomenon apparently related to the occurrence of secondary flows in the metering nip. Finally, the numerical results also showed that the minimum nip gap becomes constant at high loads.

Keywords: Torque; Nip flow; Reverse coating; Rheology; Spitting

1. Introduction

The metering size press is an example of a film coating transfer technique that has received considerable attention because of its potential to coat paper webs with minimal stresses. This technique also allows to coat wood-containing paper with reduced web breaks and produces a contour-like coating with superior fiber coverage (Ahlroos, Alexandersson, & Grön, 1999). These advantages are due to a premetering step, whereby a metered film is first formed before being applied to the base paper. The understanding of the metering nip flow hydrodynamics is very important to control the metered film properties such as coating uniformity and thickness, which are related to the quality of the final product.

The film uniformity depends on the metering nip flow stability. Several studies have been carried out to characterize nip flow in coaters. For instance, Pitts and Greiller (1961) established a stability criterion based on the pressure gradient. When it is positive, the flow tends to be less prone to hydrodynamic defects such as ribbing. The capillary number has also been used to predict the onset of ribbing (Coyle, Macosko, & Scriven, 1990a, b; Carvalho & Scriven, 1997, 1999). At less than 300 m/min, Coyle et al. (1990b) showed that operating windows based on the speed ratio and the capillary number can be used to predict whether the flow will be stable to ribbing. However, to make the paper coating process economically attractive, coating stations are operated at a much higher speed, typically in the range 1000–1500 m/min. Unfortunately, at those speeds, the proposed criteria required to obtain a defect-free film cannot be applied due to significant changes in the nip flow hydrodynamics (Réglat & Tanguy, 1997, 1998; Alonso & Tanguy, 2001).

Since a stable flow cannot be obtained at high speed, other aspects such as the nip geometry and the rheology of the coating colors become key issues in obtaining a film as uniform as possible. A smaller metering rod helps to stabilize the flow by creating a flatter meniscus at the nip delivery (Ruschak, 1982). The use of a deformable cover is also known to reduce the rib width and delay the onset of ribbing (Carvalho & Scriven, 1999). At high speed, the metering rod speed seems to have a negligible effect on the ribs, but increasing the rod load decreases rib width (Réglat

* Corresponding author. Tel.: +1-514-340-4017; fax: +1-514-340-4105.
E-mail address: philippe.tanguy@polymtl.ca (P. A. Tanguy).
[1] Present address: CIATEC, A.C., Omega 201, Fracc. Ind. Delta, C.P. 37520, Leon, Gto., Mexico.

0009-2509/03/$ - see front matter © 2003 Elsevier Science Ltd. All rights reserved.
doi:10.1016/S0009-2509(03)00009-5

& Tanguy, 1998; Alonso & Tanguy, 2001) facilitating the rib leveling.

Along with the coater technology, the coating color properties influence the coating process hydrodynamics. As coating speed increases, the solids content of the coating fluid must be increased to meet the drying capacity of the coating machine. A higher solids content means higher viscosity, so that wider ribs are created (Réglat & Tanguy, 1998; Alonso & Tanguy, 2001), although there is a smaller tendency for the fluid to spit off the rod (Alonso & Tanguy, 2001; Grön, Sunde, & Nikula, 1998). At high speed, a wider nip gap is also generated (Alonso & Tanguy, 2001); hence a thicker coating is produced. Higher loads are then required to maintain the target coating thickness by reducing the nip gap. It also comes as no surprise that, in the metering nip, the conditions of very high shear during a very short period of time require a full rheological characterization of the coating colors. The knowledge of the coating "rheological state" leaving the metering nip is needed to understand what occurs in the application nip where undesirable phenomena such as misting and orange peel may appear (Grön et al., 1998; Alonso, Bertrand, Réglat, Choplin, & Tanguy, 2001a).

High-speed coating requires the use of a deformable roll cover to avoid the rolls from clashing (Carvalho & Scriven, 1997). The deformable cover also contributes to the coater performance in terms of equipment wear, thermal effects, and film splitting (Moore, 1999). Furthermore, it directly affects the nip pressure behavior in such a way that decreased pressure gradients are produced (Carvalho & Scriven, 1999) resulting in a more stable flow and a more uniform film.

When a deformable cover is used, a solid-fluid boundary is generated with an a priori unknown shape. As a result, the rod-roll clearance cannot be measured but only estimated (Alonso, Réglat, Bertrand, & Tanguy, 2000; Alonso, Bertrand, & Tanguy, 2001b). The numerical modeling of the cover deformation then helps to understand the effects of the roll hardness and the cover thickness on the hydrodynamics of the flow (Coyle, 1988; Carvalho & Scriven, 1999; Cohu & Magnin, 1997). Among all the investigations reported in the literature, however, only a few have relied on the use of an elastohydrodynamic model (Fourcade, Bertrand, Réglat, & Tanguy, 1999; Carvalho & Scriven, 1997, 1999; Alonso et al., 2001a, b).

To assess the reliability of computer modeling in such a context, the use of parameters that are particularly sensitive to the nip elastohydrodynamic forces, such as the torque acting on the rotating rod, becomes natural. Torque measurements are at the basis of rotational rheometry (Macosko, 1994; Carreau, De Kee, & Chhabra, 1997) and they can also be adapted to mixing process rheometry (Brito-de la Fuente et al., 1998). From a fluid mechanics viewpoint, we believe that the torque signal may provide relevant information about the hydrodynamic conditions of the fluid in the metering nip, in the same spirit of what has been obtained from experimental pressure measurements (Réglat & Tanguy, 1998; Alonso et al., 2000, Alonso & Tanguy, 2001, Alonso et al., 2001a, b). Consequently, the objective of this work is to investigate the metering nip flow hydrodynamics by using the metering rod torque signal. Numerical results are compared to experimental measurements to better understand the effect of the transfer speed on both the torque signal and coater runnability.

2. Experimental work

The laboratory reverse roll coater used in the experiments (Fig. 1 and Table 1) has already been described elsewhere (Réglat & Tanguy, 1997; Alonso & Tanguy, 2001). Briefly, the metering rod of the coater is instrumented with a

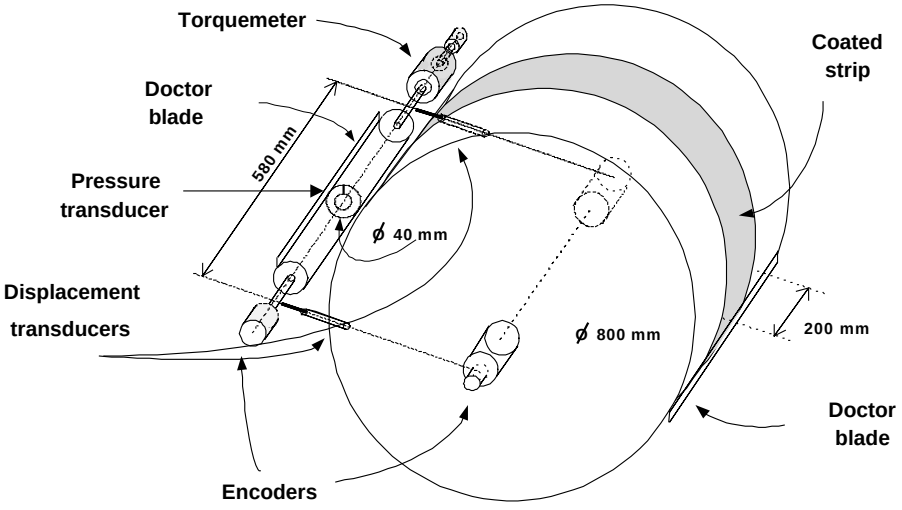

Fig. 1. Instrumentation of the metering section of the laboratory coater.

Table 1
Operating and geometrical parameters

Parameter	Nomenclature	Range
Transfer speed	V_t	500–1900 m/min
Metering rod speed	V_m	30 m/min
Metering load	—	0.25–1.5 kN/m
Transfer roll diameter	r_t	0.80 m
Metering rod diameter	r_m	0.04 m
Elastomer thickness	t_e	0.015 m
Metering nip length	l	0.02 m
Metered coated strip	—	0.2 m

wall-mounted piezoelectric transducer (response frequency of 250 kHz) and allows obtaining the nip pressure profile at each rotation. A pressure profile is an average of ten consecutive profiles and it is obtained by computing the mean value at each acquired data point. The maximum uncertainty of this profile is 2% full scale, within a 95% confidence limit and is reproducible within a range of 3% full scale (Réglat & Tanguy, 1997). Likewise, two displacement transducers located at each end of the rod measure at any time the relative position of the metering rod with respect to the undeformed surface of the transfer roll (the zero position is set when** both rod and roll are in slight contact at rest). This position is approximately defined by the naked eye, with an uncertainty of ±20 μm (Réglat & Tanguy, 1997). Then all the measurements are fitted with the same bias, but repeatability gives a relative uncertainty of ±3 μm. A torquemeter is directly connected to the shaft of the metering rod so that the torque signal is recorded continuously. The maximum torque measurable by the torquemeter is 1.4 N m and its accuracy is 0.5% full scale. By resetting all the parameters, the viscosity, the position on the rod, and the speeds of both roll and rod, the torque values are reproducible within a range of 6% full scale.

Spitting and air entrapment were assessed by means of high-speed visualization using a video system. Recordings of the metering film were taken and the onset of spitting was detected visually with the appearance of the first droplets.

Polyethylene glycol solutions at two concentrations (13.2%, 17% w/w) were used as Newtonian fluids. Three paper coating color formulations were also tested, all based on 100 dry parts of clay, 10 of latex, 0.04 of dispersant, with different CMC and solids contents as shown in Table 2. The Cross model was used to fit the flow curves of these coating colors and the rheological parameters were obtained by non-linear regression (Table 3). Details about the rheological characterization and the Cross model can be found elsewhere (Alonso & Tanguy, 2001; Alonso et al., 2001a, b).

Table 2
CMC and solids content in the coating colors

Coating color	CMC	% Solids
1	0.5	61.0
2	1.0	61.0
3	0.5	63.3

3. Numerical model

The numerical results presented in this paper were obtained following the finite element procedure described in Fourcade et al. (1999) and Alonso et al. (2001b). In the computational approach, the fully flooded fluid problem is first solved with a fluid–solid interface corresponding to that of a non-deformed transfer roll. Normal stresses are calculated to evaluate the normal force exerted by the fluid on the transfer roll surface. Tangential stresses are used to calculate the tangential force exerted by the fluid on the metering rod. The transfer roll surface deformation is then predicted from static analysis and the solid–fluid interface is modified accordingly. This new modified fluid–solid interface is used in the next iteration and the iterative process is continued until the change in the normal forces at the interface becomes sufficiently small. A relaxation technique is used to smooth the iterative procedure and speed up convergence. Once the problem has converged for a set of parameters P, it is possible to find another solution for a new set of parameters Q (if either the viscosity, the nip gap, the transfer or the metering speeds are modified). In such a case, the fluid–solid interface of the solution corresponding to P can be used as the initial interface shape for finding the new solution corresponding to Q. In this manner, negative metering rod positions can be managed if the transfer roll cover is sufficiently compressed to allow room for the displacement of the rod towards the roll. This technique has already been used in similar elastohydrodynamic problems (Carvalho & Scriven, 1997, 1999; Fourcade et al., 1999). In the present investigation, the two-dimensional elastohydrodynamic problem was discretized with the Galerkin finite element method by means of CFD code POLY2D^{TM} (Rheotek Inc.) The meshing procedure was achieved using IDEAS^{TM} (SDRC Inc.) Both fluid and solid meshes contained around 3400 and 4800 quadratic triangular elements, respectively. Mesh refinement tests were performed to ensure that the results were independent of the mesh size. The remeshing procedure was such that the variation of the number of elements did not change appreciably through the iterations [± 2%].

4. Results and discussion

4.1. Minimum nip gap behavior

Fig. 2(a) shows the change in the minimum nip gap with respect to the metering rod position for colors 2 and 3, as predicted from the simulations. A linear behavior is obtained

Table 3
Parameters of cross model $\mu_{Cross} = \eta_\infty + [\eta_0 - \eta_\infty]/[1 + (t\dot{\gamma})^p]$

Coating color label	t (s)	p	η_0 (Pa s)	η_∞ (Pa s)	$\lvert(\mu_{exp} - \mu_{Cross})/\mu_{Cross}\rvert$
1	87	0.84	500	0.063	0.083
2	62.5	0.83	500	0.082	0.095
3	83	0.82	500	0.080	0.094

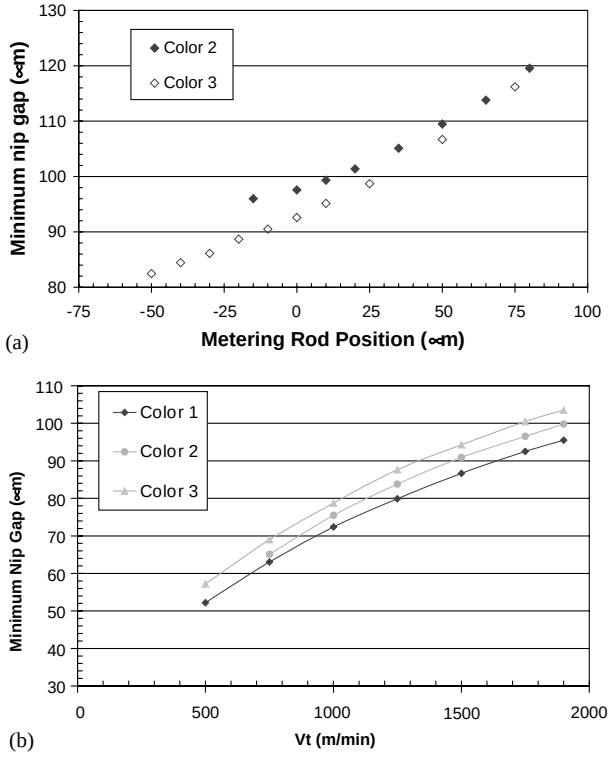

Fig. 2. (a) Numerical minimum nip gap vs. metering rod position ($V_t = 1750$ m/min, $V_m = 30$ m/min). (b) Numerical minimum gap vs. transfer speed for a metering rod position of 15 μm ($V_m = 30$ m/min).

at low loads (large values of the minimum nip gap), when the deformation of the transfer roll is minimal (Carvalho & Scriven, 1997, 1999). This behavior, however, becomes non-linear at high loads (narrow gaps) and tends to level off to a constant value at very high loads. This same nip gap behavior has been reported in the literature at low speed (Coyle, 1988, Carvalho & Scriven, 1997, 1999). The constant minimum nip clearance at very high loads also complies with experiments in which the coating thickness was kept constant (Grön et al., 1998). The negative metering rod positions of Fig. 2(a) were obtained by starting from a non-deformed case with a positive nip gap (the zero corresponds to contact with a non-deformed cover) and by using the predicted deformed state as an initial condition for subsequent simulations. By doing so, it was thus possible to decrease the rod position to small and even negative (the distance between the rod and roll axes is smaller than the sum of both rod and roll radii) values.

The minimum nip gap seems to exhibit a non-linear behavior with respect to the transfer speed, as shown in Fig. 2(b) for colors 1–3 at a metering rod position of 15 μm. It is different from experiments reported in the literature, where the relative position of the metering rod is a linear function of the transfer speed (see Réglat & Tanguy, 1997, 1998). One possible reason for this discrepancy is the hydrodynamic equilibrium that takes place in the experimental nip, where the load on the rod is imposed so that the position of the metering rod depends on this hydrodynamic balance. In the numerical simulations, on the other hand, the rod position is imposed as a boundary condition; this means that the changes in the nip gap are the result of the hydrodynamic equilibrium between the flow and elastic forces in the nip. Experimentally, the nip clearance cannot be measured, but only estimated (Alonso et al., 2001b).

4.2. Torque signal

The variation of the tangential force with respect to the position in the nip is shown in Fig. 3(a). It appears that the tangential force profile is very sensitive to the color shear-thinning index p. As the pseudoplastic behavior increases (shear-thinning index departing from zero), both viscosity and torque decrease. Simultaneously, as shown in Fig. 3(b), the secondary flow located upstream from the nip becomes smaller and flattens out, owing to an increase of inertia (note that the deformation of the roll cover does not appear on the graph at such a scale). Although the existence of these recirculations has already been predicted (Coyle et al., 1990a, b), it can be observed here that the negative values of the tangential forces are in phase with the recirculations. We may therefore advocate that the negative torque values upstream from the nip may originate from the secondary flows. The drag from the transfer roll on the coating color is such that the rotation speed of the vortex is higher than the rod speed.

The pressure profile for the shear-thinning fluid with a flow index value of 0.5 is also shown in Fig. 3(a). It complies with the pressure profile found in the literature for a fully flooded nip when a deformable transfer roll cover is used (Carvalho & Scriven, 1997; Fourcade et al., 1999.) Because the free surface was not taken into account in our simulations, the computed sub-atmospheric pressure downstream of the nip is overestimated and reaches unrealistic

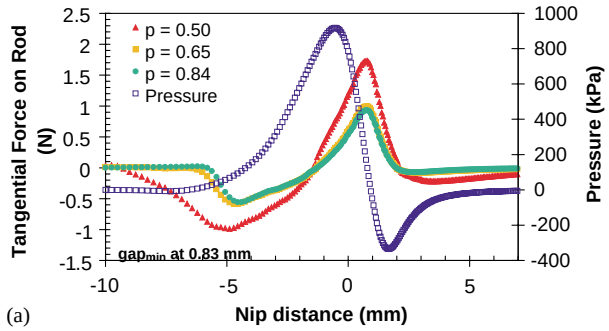

(a)

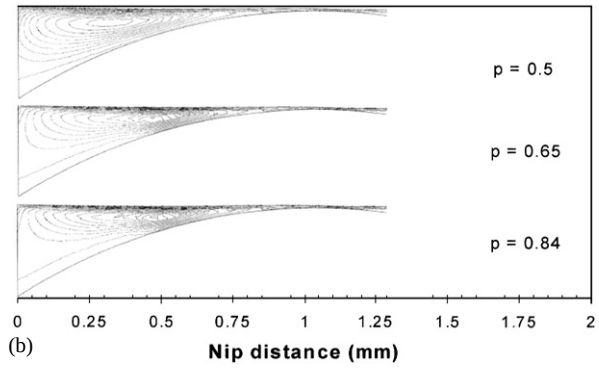

(b)

Fig. 3. (a) Numerical tangential force and pressure profiles vs. the nip distance for different values of the shear-thinning index ($V_t = 1750$ m/min, $V_m = 30$ m/min, metering rod position = 10 μm). (b) Flow profiles (streamlines) in the metering nip (Reynolds number increases from top to bottom; $V_t = 1750$ m/min, $V_m = 30$ m/min, metering rod position = 10 μm).

values. This spurious phenomenon would disappear if the free surface was accounted for (Fourcade, Bertrand, & Tanguy, 1998), but the simultaneous consideration of both the free surface and roll deformation is beyond the present capabilities of our code. Near the nip center, the change in the slope coincides with the maximum tangential force on the rod. The minimum nip gap is located at the position where the maximum values of the shear and the rod tangential force take place. The nip gap profile (not shown here) is very similar to the results found in the literature (Carvalho & Scriven, 1997).

Fig. 4 shows the very complex relationship between the experimental torque and the transfer speed obtained for coating color 2 (according to the constructor specifications, the maximum error on the torque values is 0.007 N m). The data points where spitting and air entrapment were observed are labeled appropriately. At low speeds and low loads, the torque increases linearly with the transfer speed. Then it becomes more and more non-linear and eventually levels off as the speed is increased, owing to the occurrence of spitting and air entrapment at wide nip gaps (low loads). When air entrapment occurs, the fluid–air mixture has a lower viscosity than that of the fluid alone and, as a result, the torque on the rod, which is nothing but the integral of the curve shown in Fig. 3(a), decreases. For intermediate load

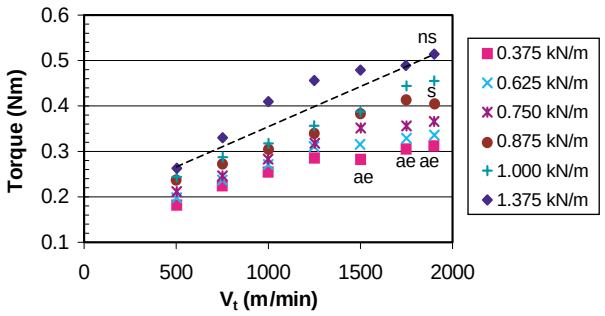

Fig. 4. Experimental torque values vs. transfer speed for different loads on the metering rod (coating color 2: ae = air entrapment, s = spitting observed, ns = no spitting observed; $V_m = 30$ m/min).

values (e.g. 0.875 kN/m), the linear behavior extends without spitting to the high-speed region due to a reduced nip clearance. However, at 1900 m/min, spitting is observed, which results in a smaller torque value. At very high loads and low speeds, that is under conditions yielding very narrow nip gaps and thin films, a dry contact between the extremities of the metering rod and the roll surface occurs (i.e. lack of coating fluid and no cover deformation) because the rod is wider than the coating head. Finally, upon increasing the transfer speed, the roll drags more and more fluid into the nip. As a result, the nip gap widens, the friction at the edges of the rod reduces and so does the experimental torque. A dotted line was drawn around the data at high loads in order to represent where they should lie if they followed the same trend than those at low loads. The lack of lubrication at the rod extremities (diamond above the dotted line) produces the excessive torque shown in Fig. 4 at intermediate speeds. This phenomenon dies out at high speeds. From these results, it can be seen that torque measurements can predict runnability problems such as air entrapment and spitting and excessive loads that may result in damaging the deformable roll cover in the regions of poor lubrication.

Fig. 5 shows, for Newtonian fluids, a comparison between the calculated and experimental torque values with respect to the transfer speed. To ensure similar hydrodynamic conditions in terms of the rod-roll clearance (we recall that the exact clearance is unknown in the experiments), the maximum pressure value was used as a basis for the comparison. In other words, the numerical and experimental torque values were compared when the experimental and numerical maximum pressure values in the nip were equal (Alonso et al., 2001a). It can be seen in Fig. 5 that the numerical and experimental curves agree fairly well at low speed. At higher speeds, however, the experimental measurements depart from the numerical results, an indication of a drag reduction phenomenon on the rod. In the experiments, the torque measured decreased when the amount of bubbles in the liquid increased. The bubbles come from air entrapment in the nip (spitting is not observed with Newtonian fluids), a phenomenon not observed at speeds lower than

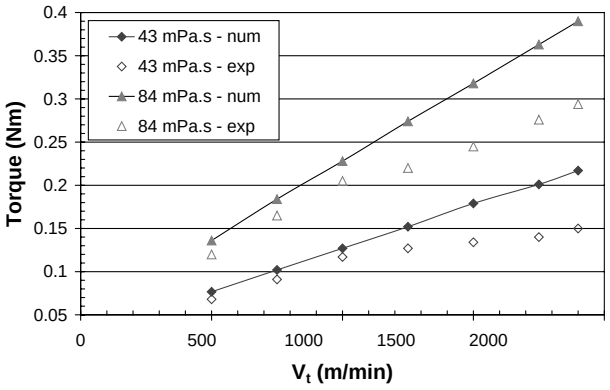

Fig. 5. Numerical and experimental torque values for Newtonian fluids ($V_m = 30$ m/min).

1000 m/min unless a wide gap superior to 100 μm (Réglat & Tanguy, 1998) is used. The bubbles entrapped in the nip produce a drag reduction on the rod that may be responsible for a decrease in the bulk viscosity of the Newtonian fluid. However, from our experience with Newtonian polyethylene glycol solutions and from the literature (Greiffenberg, Lohmander, & Rigdahl, 1999), it seems that the presence of bubbles tends to increase the viscosity measured in the rheometer. Neither these authors nor us have performed an analysis of the bubble size. We believe that the viscosity of the fluid not only depends on the amount of air entrapped in the liquid, but on the size of the bubbles as well.

Fig. 6(a) compares the numerical and experimental torque values for coating colors 1 and 2. Here again, spitting was observed for the highest transfer speeds (the data points on the graph have been labeled when appropriate.) Contrary to Newtonian fluids, the increased viscosity of the coating colors at low shear rates (shear-thinning behavior) decreases significantly the air entrapment in the nip, although the air content in the coating color may still be a problem (Greiffenberg et al., 1999). At low speed, the numerical and experimental torque curves are different but almost parallel. The deviation can be explained by a possible particle slippage phenomenon along the rod. The difference between the experimental and numerical torque values becomes larger with the speed, particularly when spitting sets in.

For coating color 3 (Fig. 6(b)), the experimental and numerical torque values superimpose at low speeds. At very high speeds, however, the experimental torque values depart from the numerical straight line, most likely owing to the observed spitting (the "**s**" labeled points on the graph). From the observations made for Newtonian fluids and coating colors 1 and 2, we expected a large discrepancy between the numerical and experimental curves at low speeds. The experimental torque values seem to be higher than expected, which suggests that coating color 3 looses some of its shear-thinning character in the nip (Alonso et al., 2001a). This particular behavior may be due to an increase in the viscosity in the nip, which is the typical rheological

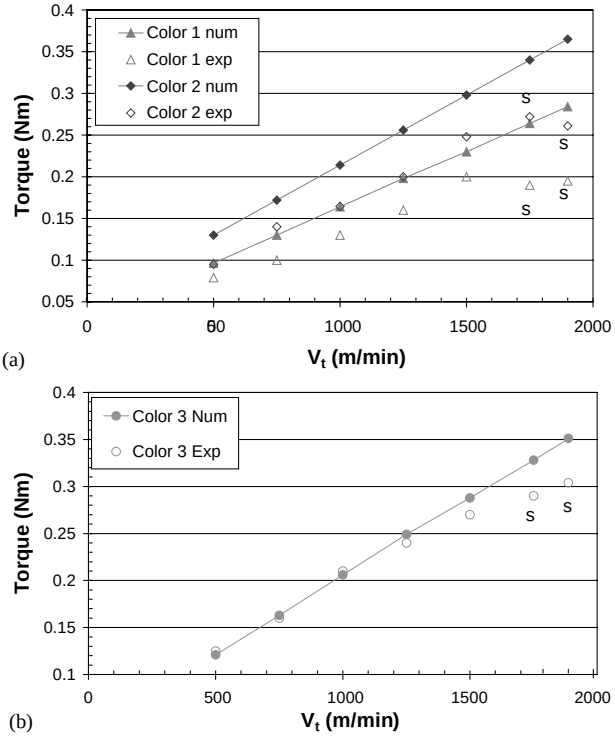

Fig. 6. (a) Numerical and experimental torque values for coating colors 1 and 2 ($V_t = 1750$ m/min, $V_m = 30$ m/min; s = spitting observed). (b) Numerical and experimental torque values for coating color 3 ($V_t = 1750$ m/min, $V_m = 30$ m/min; s = spitting observed).

behavior for a suspension with high solids content under very high shear rates (Roper & Attal, 1993). This growth in viscosity (a shear-thickening behavior not observed in the rheometer) has been explained in terms of particle collisions at very high shear rates (Roper & Attal, 1993). In the nip, shear stresses can be such that particles collide, increasing the internal resistance of the coating color to flow. This may be the case for color 3 (higher solids content), resulting in an increased viscosity in the nip and an experimental torque value higher than expected (Alonso et al., 2001a).

Another possible explanation is related to the viscoelastic nature of coating colors at low deformation (Carreau & Lavoie, 1993; Alonso et al., 2001a). It makes no doubt that, if present, elasticity would increase the torque, in which case the extensional rates along the rod would be significant. Shear-induced elasticity has been associated with shear-thickening behavior in the literature (Laun & Hirsch, 1989) so that these effects might be present for coating color 3.

Slippage effects may lessen the torque signal if they are significant. Drag reduction owing to particle migration has been observed in a Couette geometry (Tetlow et al., 1998), but it has not been observed in the metering nip. Surface roughness affects the wall slip behavior of a suspension and may be conveniently used to prevent it (Aral & Kalyon, 1994). Consequently, the finish of the metering rod could be modified to decrease the slippage on the rod and thus

improve the torque measurements. Clarifying the importance of these effects is clearly an interesting topic for future research.

5. Conclusion

We showed in this investigation that torque measurements could be used to predict runnability problems such as air entrapment and spitting. It was found that the torque increases with transfer speed, load and viscosity. For coating colors, when runnability problems such as spitting are observed, the torque signal decreases. Torque measurements can also be used to predict excessive friction between the rod and roll edges, showing the importance of lubricating the nip extremities. Furthermore, the numerical simulations showed trends similar to those of the experiments. A negative torque value can be associated to a phenomenon whereby the fluid enhances the motion of the metering rod. This phenomenon may be related to the appearance of secondary flows in the metering nip. The numerical minimum nip gap complies with the observations reported in the literature, showing that the film coating thickness becomes constant at very high loads. From all these findings, it is concluded that the metering rod torque signal can provide relevant information about the metering flow hydrodynamics and some of the spurious phenomena that are generated.

Acknowledgements

The financial contributions of Paprican and NSERC (Canada), and CONACYT (Mexico) are gratefully acknowledged.

References

Ahlroos, J., Alexandersson, M., & Grön, J. (1999). Influence of base-paper filler content and precalendering on a metered film press coating-paper and print quality. *Tappi Journal*, *82*, 94–100.

Alonso, S., Bertrand, F., Réglat, O., Choplin, L., & Tanguy, P. A. (2001a). Process viscosity in reverse roll coating. *Chemical Engineering Research and Design*, *79*, 128–136.

Alonso, S., Bertrand, F., & Tanguy, P. A. (2001b). A CFD assessment of film coating process viscosity models. *Canadian Journal of Chemical Engineering*, *79*, 751–759.

Alonso, S., Réglat, O., Bertrand, F., & Tanguy, P. A. (2000). Process viscosity in a film coater. *Paperi ja Puu (Paper and Timber)*, *82*, 34–40.

Alonso, S., & Tanguy, P. A. (2001). Hydrodynamic instabilities in the metering nip of a film coater. *Tappi Journal*, *84*, 67 + electronic document (20 pp.)

Aral, K. B., & Kalyon, D. M. (1994). Effects of temperature and surface roughness on time-dependent development of wall slip in steady torsional flow of concentrated suspensions. *Journal of Rheology*, *38*, 957–972.

Brito-de la Fuente, E., Nava, J. A., Lopez, L. M., Medina, L., Ascanio, G., & Tanguy, P. A. (1998). Process viscosimetry of complex fluids and suspensions with helical ribbon agitators. *Canadian Journal of Chemical Engineering*, *76*, 689–695.

Carreau, P. J., De Kee, P., & Chhabra, R. P. (1997). *Polymer rheology*: *Principles and applications*. Munich: Hanser Editors.

Carreau, P. J., & Lavoie, P. A. (1993). Rheology of coating colors: A rheologist point of view. *Proceedings of the Tappi advanced coating fundamentals symposium*, Minneapolis (pp. 1–12).

Carvalho, M. S., & Scriven, L. E. (1997). Deformable roll coating flows: Steady state and linear perturbation analysis. *Journal of Fluid Mechanics*, *339*, 143–172.

Carvalho, M. S., & Scriven, L. E. (1999). Three-dimensional stability analysis of the free surface flows: Application to forward deformable roll coating. *Journal of Computational Physics*, *151*, 534–562.

Cohu, O., & Magnin, A. (1997). Forward roll coating of Newtonian fluids with deformable rolls: an experimental investigation. *Chemical Engineering Science*, *52*(8), 1339–1348.

Coyle, D. (1988). Forward roll coating with deformable rolls: A simple one-dimensional elastohydrodynamic model. *Chemical Engineering Science*, *43*, 2673–2684.

Coyle, D., Macosko, C. W., & Scriven, L. E. (1990a). Stability of symmetric film-splitting between counter-rotating cylinders. *Journal of Fluid Mechanics*, *216*, 437–458.

Coyle, D., Macosko, C. W., & Scriven, L. E. (1990b). The fluids dynamics of reverse roll coating. *AIChE Journal*, *36*, 161–174.

Fourcade, E., Bertrand, F., Réglat, O., & Tanguy, P. A. (1999). Finite element analysis of fluid-solid interaction in the metering nip of a metering size press. *Computational Methods in Applied Mechanics and Engineering*, *174*, 235–245.

Fourcade, E., Bertrand, F., & Tanguy, P. A. (1998). Numerical modeling of the hydrodynamics in the metering nip of a film coater. *Computer fluid dynamics society of Canada*, *sixth annual conference*, Quebec. V (pp. 17–22).

Greiffenberg, I., Lohmander, S., & Rigdahl, M. (1999). Effects of the air content on the rhelogical properties of coating colors. *Tappi advances coating fundamentals symposium proceedings* (pp. 149–156). Tappi Press, Minneapolis.

Grön, J., Sunde, H., & Nikula, E. (1998). Runnability aspects in high speed film transfer coating. *Tappi Journal*, *81*, 157–165.

Laun, H. M., & Hirsch, G. X. (1989). New laboratory tests to measure rheological properties of paper coatings in transient and steady-state flows. *Rheologica Acta*, *28*, 267–280.

Macosko, C. W. (1994). *Rheology, principles, measurements, and applications* (p. 78). New York: VCH Publishers.

Moore, R. R. (1999). Influence of roll covers in film transfer nip presses and coaters. *Tappi Journal*, *82*, 111–114.

Pitts, E., & Greiller, J. (1961). The flow of thin liquids films between rollers. *Journal of Fluid Mechanics*, *11*, 33–50.

Réglat, O., & Tanguy, P. A. (1997). A experimental study of the flow in the metering nip of a metering size press. *AIChE Journal*, *80*, 2911–2920.

Réglat, O., & Tanguy, P. A. (1998). Rheological investigations of $CaCO_3$ slurries in the metering nip of a metering size press. *Tappi Journal*, *81*, 195–205.

Roper, D. A., & Attal, J. F. (1993). Evaluations of coating high-speed runnability using pilot plant coater data, rheological measurements, and computer modeling. *Tappi Journal*, *76*, 55–62.

Ruschak, K. J. (1982). Boundary conditions at a liquid/air interface in lubrication flows. *Journal of Fluid Mechanics*, *119*, 107–120.

Tetlow, N., Graham, A. L., Ingber, M. S., Subia, S. R., Mondy, L. A., & Altobelli, S. A. (1998). Particle migration in a Couette apparatus: Experiment and modeling. *Journal of Rheology*, *42*, 307–327.